SINTERING EFFECTS ON MICROSTRUCTURE AND ELECTRICAL PROPERTIES OF $CaCu_3Ti_4O_{12}$ CERAMICS

S. Marković[1], M. Lukić[1], Č. Jovalekić[2], S.D. Škapin[3], D. Suvorov[3] and D. Uskoković[1]
[1]Institute of Technical Sciences of the Serbian Academy of Sciences and Arts, Belgrade, Serbia
[2]Institute for Multidisciplinary Research, Belgrade, Serbia
[3]Jožef Stefan Institute, Ljubljana, Slovenia

ABSTRACT

CCTO powders were prepared by solid state reaction and mechanochemically, respectively. Synthesized powders were characterized by XRD, FE–SEM and PSA techniques. The sinterability of CCTO powders was investigated by heating microscopy. Powders were uniaxially pressed into pellets and sintered up to 1100 °C, with heating rates of 2, 5, 10 and 20 °/min. The recorded shrinkage curves were used for choosing conventional and two step sintering (TSS) conditions. By TSS the samples were heated up to 1070 °C and after retention for 10 min cooled down to 1020 °C and kept for 20 h. The microstructure of CCTO ceramics sintered by conventional and TSS techniques was examined by FE–SEM method; the electrical properties were investigated in medium frequency (MF) range (42 Hz–5 MHz) and in the microwave (MW) range of frequencies. Electrical properties of the sintered CCTO ceramics were correlated to the samples microstructure. Finally, we have shown that appropriate choice of sintering conditions is important for preparation of high-quality CCTO ceramics with high dielectric permittivity in the kilohertz range as well as at the resonant frequency.

INTRODUCTION

Calcium copper titanate ($CaCu_3Ti_4O_{12}$, CCTO) belong to a group of $ACu_3B_4O_{12}$ perovskite-type compounds,[1] which attracted ever-increasing attention for its practical applications in microelectronics, especially for preparation of capacitors and memory devices. CCTO ceramics are very attractive because of their giant dielectric constant ($\sim 10^4$–10^5) in the kilohertz region at room temperature, and their good stability over a wide temperature range from 100 to 600 K. Reasons for interesting electrical properties of CCTO-type materials are not fully understood, and during the years different theoretical models and suggestions have been proposed to explain this behavior. However, since the giant dielectric properties primarily depend on the grain boundary resistivity while an intrinsic mechanism is excluded, ceramic microstructure (i.e. the average grain size and pellet density) and processing conditions (such as the oxygen partial pressure, sintering temperature, and cooling rate) are very important.[2,3] It is shown that varying sintering parameters desired electrical properties could be tailored.[4] Solid state reaction and mechanochemical treatment have been widely used as simple and fast synthesis methods. Having this in mind, designing appropriate processing route for such CCTO powders to achieve dense electroceramics with high dielectric permittivity and its stability in wide temperature range is desired. Until now, TSS method has been used for processing of sol-gel derived CCTO ceramics and method applicability for grain growth suppression at level of 6 μm is shown.[5]

In this paper, CCTO powders were prepared by solid-state reaction and mechanochemically, respectively. Synthesized powder was characterized by XRD, FE–SEM and PSA techniques. The sinterability of CCTO powders was investigated by heating microscopy. Powder was uni-axially pressed into pellets (∅ 6.7 mm) and sintered up to 1100 °C, with heating rate of 2, 5, 10 and 20

°/min. The recorded shrinkage curves were used for choosing of further sintering conditions, conventional as well as two-step sintering. The microstructure and electrical properties of sintered ceramics were examined and obtained results were correlated.

EXPERIMENTAL PROCEDURE

The polycrystalline calcium copper titanate ($CaCu_3Ti_4O_{12}$, CCTO) powders were prepared by two different techniques: (1) solid-state reaction and (2) mechanochemically by high-energy ball milling. In both cases the starting materials were commercially available powders of high purity: calcium carbonate ($CaCO_3$) (>99 %, Centrohem, Serbia), copper oxide (CuO) (>99%, Kemika, Zagreb) and titanium oxide (TiO_2) (>99.8%, Ventron GmbH, Germany) in a stoichiometric ratio $CaCO_3$–$3CuO$–$4TiO_2$. For solid-state reaction synthesis, mixture of the starting powders was homogenized during 24 hours in isopropanol under constant stirring at 1000 rpm. After that powder slurry was filtered, dried and calcined at 1000 °C for 12 hours. Calcined powder was grinded in agate mortar with addition of isopropanol and XRD pattern was recorded. The process of calcination and grinding was repeated several times until the formation of CCTO compound was confirmed by XRD studies. For the mechanochemical synthesis the powders mixture was grinded in a Fritsch Pulverisette 5 planetary ball mill. Milling was performed with tungsten carbide balls (Ø 10 mm) and sealed vials (250 ml). The mass of the powder was 6.5 g and the balls-to-powder mass ratio was 40:1. The milling was done in air atmosphere without any additives for 5 h. The angular velocities of the supporting disk and vials were 317 and 396 rpm, respectively. The milling vessels were opened every hour for removing the water vapor overpressure, since the temperature of the vessel was over 120 °C during the milling process. Overpressure of gases in the vessel reduced the efficiency of milling, especially in the case of water vapor.

The reaction occurring at high temperature or during milling can be summarized as:

$$CaCO_3 + 3\ CuO + 4\ TiO_2 \rightarrow CaCu_3Ti_4O_{12} + CO_2$$

CCTO powders synthesized by solid-state reaction and mechanochemically were denoted as CCTO_ss and CCTO_mc, respectively.

The phase composition of the synthesized CCTO powders and sintered ceramics was determined according to X-ray diffraction (XRD) data. XRD patterns were obtained at room temperature using a Philips PW-1050 automated diffractometer with Cu tube ($\lambda_{CuK\alpha}$ = 1.54178 Å); the X-ray generator operated at 40 kV and 20 mA. The diffraction measurements were done over scattering angle 2θ from 10 to 70 ° with a scanning step size of 0.05 °. JCPDS database[6] was used for phase identification. The particle size distribution was determined by the particle size analyzer Mastersizer 2000 (Malvern Instruments Ltd., UK).

The synthesized CCTO powders were uniaxially pressed in die (∅ 6.7 mm) under a pressure of 400 MPa; each of compacts has the thickness *circa* 2 mm. Green compacts with 60±2 % TD were prepared. The sintering of the green bodies was carried out in a Protherm tube furnace in air atmosphere, by both, conventional (CS) and two-step sintering (TSS) methods, respectively. At first, in the aim of finding the appropriate conditions for sintering, the non-isothermal sintering of the CCTO compacts was done in a heating microscope with automatic image analysis (New Heating Microscope EM201, Hesse Instruments, Germany). The non-

isothermal experiments were performed in air up to 1100 °C, using a heating rate of 2, 5, 10 and 20 °/min. The recorded shrinkage curves were used for choosing sintering conditions for further conventional (CS) and two-step sintering (TSS) experiments in the aim to prepare dense ceramics with good dielectric properties. The CS was done by the heating rate of 5 °/min up to 1050 °C; the dwell time was 12 hours. Furthermore, for TSS, the samples were heated up to T_1 (1070 °C) and after retention for 10 min at T_1, the samples were cooled down to T_2 (1020 °C) and, subsequently, kept in the second-step temperature for 20 h. The heating rate of TSS was 5 °/min, while the cooling rate, between T_1 and T_2, was 50 °C min^{-1} and after T_2, samples were naturally cooled down with the furnace to room temperature. The density of the sintered samples was estimated according to Archimedes' principle, and listed in Table I.

The morphology of the used CCTO powders and microstructure of the sintered ceramics were analyzed by field emission scanning electron microscopy (FE–SEM, Supra 35 VP, Carl Zeiss). Before the analysis, the powders were dispersed in ethanol, filtered, and carbon coated, while the sintered samples were polished and thermally etched at 1000 °C for 10 min, and afterwards carbon coated. The obtained micrographs were used for the estimation of the average grain size with a SemAfore digital slow scan image recording system (JEOL, version 4.01 demo).

The electrical characterization of CCTO ceramics was performed in medium frequency (MF) and microwave (MW) regions. For impedance measurements in MF region HIOKI 3532-50 LCR HiTESTER was used. The measurements were done in frequency interval 42 Hz–5 MHz, in air atmosphere, during cooling from 500 to 25 °C; an applied *ac* voltage was 1 V. As electrodes, high conductivity silver paste was applied onto both sides of the samples. The resonance measurements in the 10 MHz–67 GHz range were done in a conventional set up using a HP E8361C PNA Network Analyzer; measurements were done on samples without electrodes.

RESULTS AND DISCUSSION

XRD patterns of CCTO powders synthesized by solid-state reaction and mechanochemically are presented in Figure 1. The XRD measurements confirmed a perovskite phase which has the centrosymmetric structure with cubic space group *Im-3* (according to JCPDS 75-2188);[6,7] besides perovskite phase, sample prepared by solid state reaction (CCTO_ss) possesses small amount of CuO and TiO_2 while CCTO_mc sample is single-phased. The broad reflections in the XRD pattern of CCTO_mc powder indicate low crystallinity and small crystallite size, what is typical for powders prepared mechanochemically i.e. by high energy ball-milling;[8] quite contrary, high temperature of the solid-state reaction, 1000 °C, yields XRD pattern with narrower diffraction maximums which indicates better crystallinity and increase in crystallite size of CCTO_ss powder.

Furthermore, CCTO powders morphology was examined by FE–SEM analysis, Figure 2. CCTO_ss powder contained nonuniform particles with sizes from 1 to 10 μm, consolidated in large condensed agglomerates with sizes rising up to 50 μm. Large, strong agglomerates with partially sintered particles are consequence of high temperature of solid-state reaction. FE–SEM micrograph of CCTO_mc powder shows nonuniform soft agglomerates with sizes from 200 to 800 nm. Evidently, the agglomerates are consisted of particles smaller of 100 nm in average size.

While FE–SEM was used for the observation of powders morphology and estimation of particles and agglomerates sizes, the average particle size and particle size distribution were studied in details by a laser particle size analyzer (PSA). However, it is known that the success of PSA technique depends on the dispersion of the powder. Since the synthesized powders are

agglomerates of primary nanoparticles (found according to the FE–SEM micrographs), it was difficult to disperse them as individual particles; and hence, in spite of real particle size, the results presented in Figure 3 indicate size (and distribution) of agglomerates.

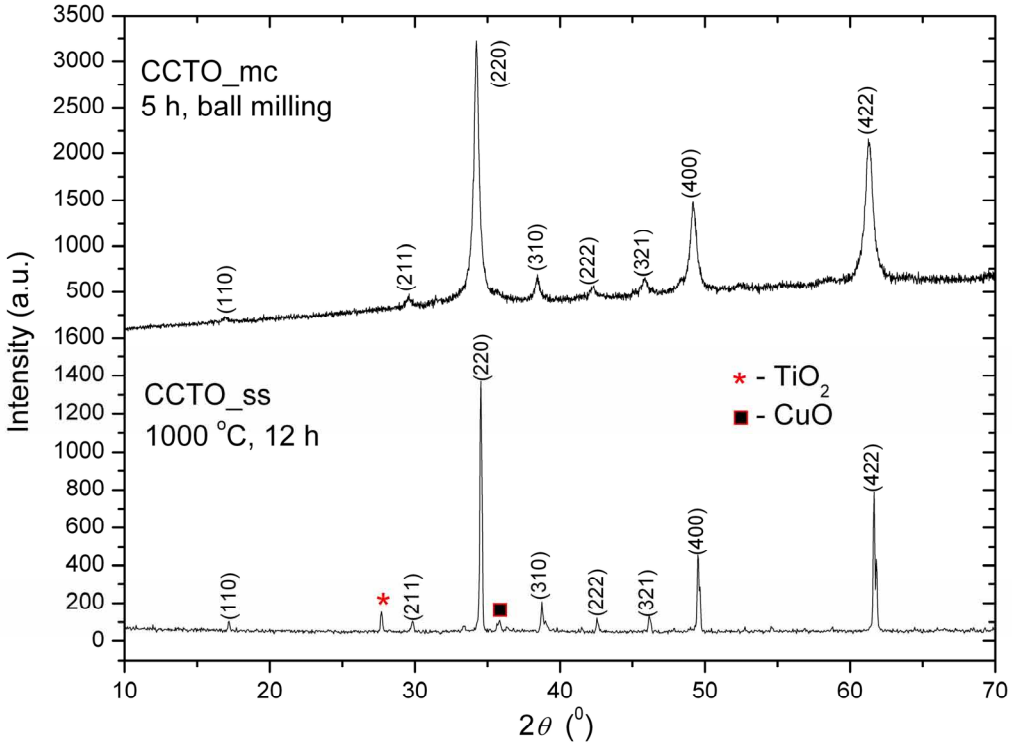

Figure 1. XRD patterns of CCTO powders synthesized by solid state reaction (CCTO_ss) and mechanochemically (CCTO_mc).

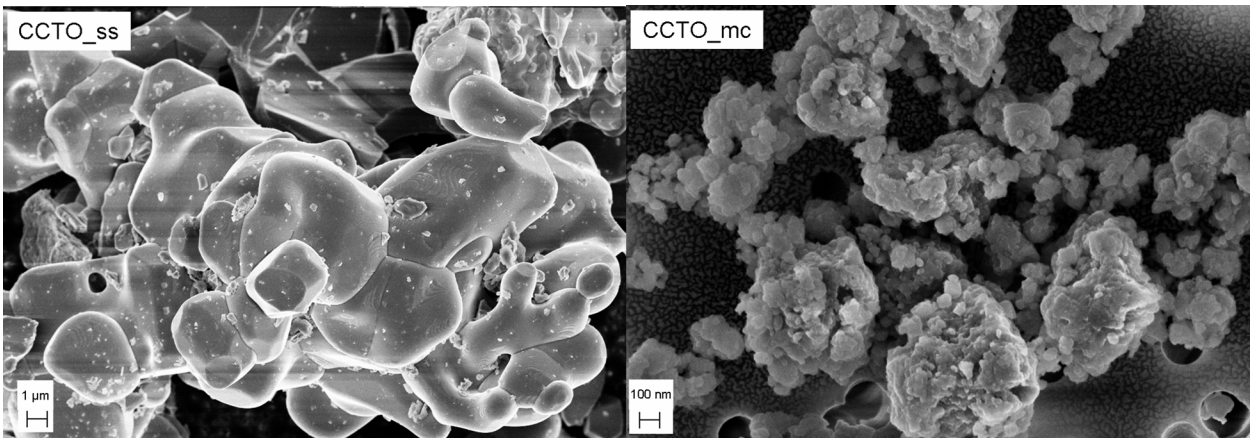

Figure 2. FE–SEM micrographs of CCTO powders synthesized by: solid state reaction (CCTO_ss) and mechanochemically (CCTO_mc).

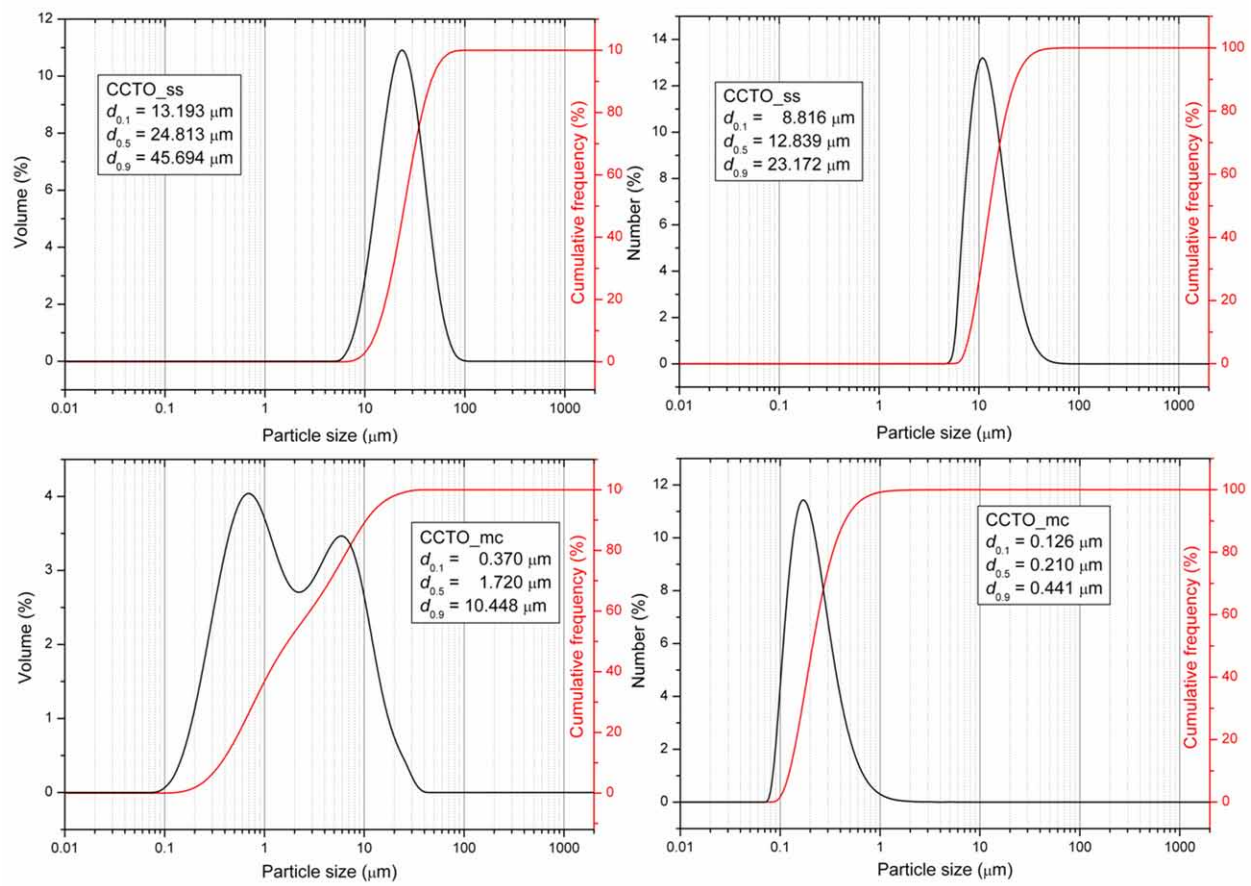

Figure 3. Particle size distribution (based on volume and number) of CCTO powders synthesized by solid state reaction (CCTO_ss) and mechanochemically (CCTO_mc).

From Figure 3, for CCTO_ss, it can be seen that particle size distributions, according to volume and number, are very narrow (*span* = 1.30 and 1.17, respectively), indicating uniform powder. From volume distribution can be seen that CCTO_ss powder possesses particles of about 25 μm in average ($d_{0.5}$), 10 % of particles ($d_{0.1}$) is smaller than 13 μm, while 90 % of particles ($d_{0.9}$) is smaller than 46 μm. Furthermore, particle size distribution according to the number shows that 10 % of particles is smaller than 8.8 μm, average particle size is 12.8 μm, while 90 % of particles is smaller than 23 μm. Thus, CCTO powder synthesized by solid-state reaction has large particles; furthermore, it can be supposed that, in average, agglomerates are consisted of two interconnected particles (grains). CCTO_mc powder shows wide (*span* = 5.86) bimodal particle size distribution based on volume. Average agglomerate size of one fraction is about 600 nm while second agglomerate fraction is about 7 μm in average. Generally, 10 % of particle agglomerates is smaller than 0.370 μm, 90 % is smaller than 10.5 μm while average size is about 1.7 μm. Quite contrary, particle size distribution according to the number is narrow (*span* = 1.50); 10 % of particles is smaller than 0.120 μm, average particle size is 0.210 μm, while 90 % of particles is smaller than 0.440 μm. Such difference between distribution according to the volume and number can be explained by a large number of small particles in CCTO_mc powder. It can be supposed that small particles (below 100 nm) are arranged in agglomerates that are basically soft in nature; besides, attractive forces between particles are weak van der Waals forces that can be easily broken down by low-intensity ultrasound.

In the second step of our investigation, the synthesized CCTO powders were pressed and sintered to prepare dense ceramics with good dielectric properties. At first, in the aim of finding the appropriate conditions for sintering, the non-isothermal sintering of the CCTO compacts was done in a heating microscope. A heating microscope was used for detailed quantitative studies of sintering as well for *in situ* monitoring of the shrinkage process; the sintering shrinkage of cylindrical compact area (A) was recorded. From the experimental data for the area recorded at 2-s time intervals during non-isothermal sintering and using equation (1), the percentage of shrinkage was calculated:

$$shrinkage\ (\%) = \frac{\Delta A}{A_o} \times 100 \qquad (1)$$

where ΔA ($=A_o - A_i$) denotes the difference between the initial value of area A_o at time t_o and the values A_i at time t_i. The calculated values of shrinkage were used for the determination of the samples' sintering behavior.

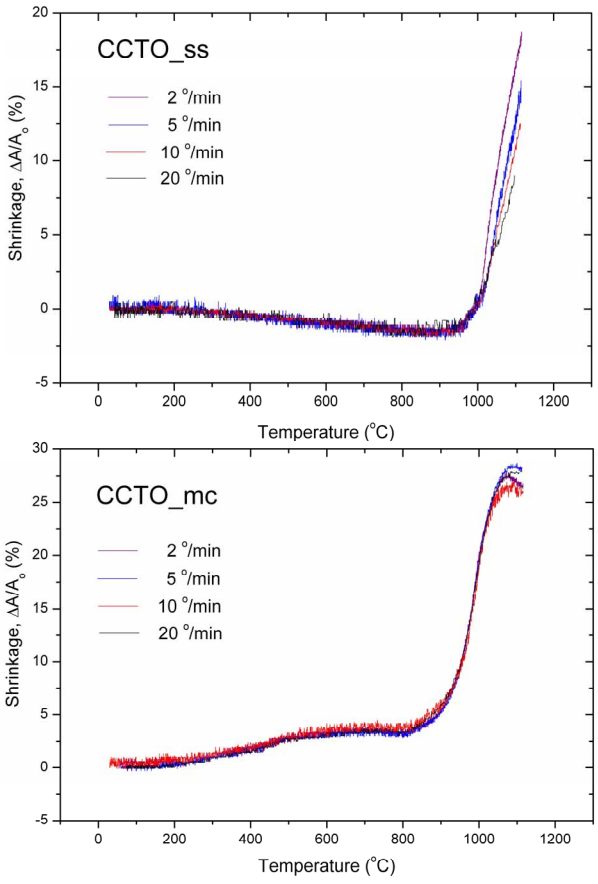

Figure 4. Shrinkage curves for CCTO_ss and CCTO_mc.

The densification of CCTO cylindrical compacts during non-isothermal sintering up to 1100 °C, using a heating rate of 2, 5, 10 and 20 °/min is represented by shrinkage curves of the samples area *versus* temperature, Figure 4.

It can be noticed that, each of the powders shows relatively similar shrinkage curves, independent on heating rate. For CCTO_ss is obvious that sintering starts at different temperatures depending on heating regime; actually, densification starts at 950 °C for slower heating and at 1050 °C for faster heating regimes i.e. delayed onset on densification with increased heating rate exists. Furthermore, CCTO_ss powder does not reach final densification stage until 1100 °C. Quite contrary, sintering curves of CCTO_mc powder are practically overlapped yielding that densification of the powder is independent on heating rate. This fact implicate good powder' sinterability. Besides, shrinkage curves show that the main densification starts at the 800 °C and reaches final stage around 1070 °C when starts to expand, probably due to forming of some eutectic melting with alumina substrate.

Thus, it can be concluded that CCTO_mc has better sinterability comparing to CCTO_ss powder, which is a consequence of powders characteristics, actually, crystallinity, average particle size and nature of agglomerates.

In the following part, according to the results of non-isothermal sintering, the conventional and two-step sintering experiments were done. Conditions for CS are chosen in the manner to obtain dense ceramics avoiding as much as possible final stage grain growth; that temperature was 1050 °C with dwell time of 12 h. Additionally, TSS sintering conditions were chosen based on sintering curves. CCTO_ss powder has very narrow temperature range of densification from 1000 to 1100 °C, while CCTO_mc powder reaches final sintering stage around 1070 °C. Since TSS method can be used for microstructural refinement and grain growth suppression, after first heating step samples should not reach final sintering stage where accelerated and uncontrolled grain growth may occur. The first sintering step should provide critical density at which interconnected pores start to collapse, while second step enables conditions for slow diffusion kinetics.[9] So, we chose 1070 °C with dwell time of 10 min for the first and 1020 °C for 20 h for the second sintering step. Heating rate of 5 °/min is chosen considering sintering curves of both CCTO_ss and CCTO_mc powders. The list of all experiments as well as characteristics of final ceramics are given in Table I.

Table I. Performed heating cycles and characteristics of final ceramics.

Powder	Heating cycle	T_1 (°C)	t_1 (min)	T_2 (°C)	t_2 (min)	Density (g/cm^3)	Average grain size (μm)
CCTO_ss	CS	1050	720	-	-	4.26	4.73
	TSS	1070	10	1020	1200	4.26	2.93
CCTO_mc	CS	1050	720	-	-	4.46	3.32
	TSS	1070	10	1020	1200	4.56	1.80

Furthermore, we used complex impedance spectroscopy (IS) to determine the electrical characteristics of CCTO ceramics tailored by different heating cycles, as well as to distinguish the grain-interior and grain boundary resistivity of the ceramics. It is known that *ac* impedance spectroscopy is a powerful tool in separating the grain-interior, grain boundary and electrode process of the ceramics.[10] In particular, a typical complex impedance diagram, in the so-called Nyquist presentation (the plot of imaginary, Z' *versus* real impedance, Z'', with the frequency f as an independent parameter) of a sintered, low-conducting material between blocking electrodes, consists of three parts (a bulk semicircle, a grain boundary semicircle, and an electrode arc), ending at the origin point of coordinate system at infinite frequency. For sintered perovskite materials, the high-frequency semicircle of the impedance spectra is attributed to the grain-interior impedance, the middle one is attributed to the grain boundary response, whereby the low-frequency arc (<0.1 Hz) corresponds to the electrode response.[11,12] The grain-interior and grain boundary resistance may be read as the diameter of appropriate arcs.

The room temperature complex impedance plots (Z^*, Z' *versus* Z'') for CCTO ceramic sintered in different heating cycles are shown in Figure 5. All Z^* plots exhibit only one arc with a large slope and the zero high frequency intercepts (see inset). Only one arc in the impedance plot is the consequence of the predominant grain boundary effect. It is known that the room temperature resistivity of perovskite materials depends mainly on the microstructural development associated with grain growth; precisely, resistivity increases with an increase of density and decrease of average grain size.[13]

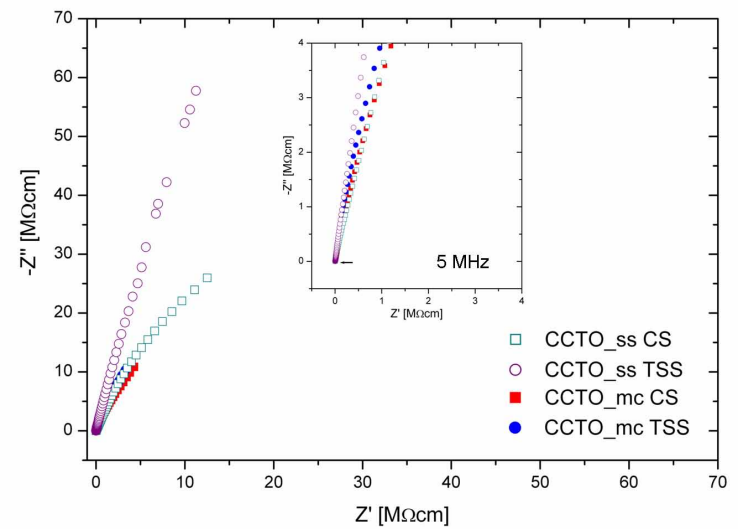

Here, it can be emphasized that IS spectra without point dissipation, indicating high-quality ceramics. This is especially important for electronic ceramics meaning no insulator interfaces (cracks and/or delamination) were produced during powders processing and high-temperature sintering.

Figure 5. Complex impedance spectra for CCTO sintered ceramics at room temperature.

From the complex impedance spectroscopy experimental data and using equation (2), the complex dielectric permittivity (ε^*) was calculated:

$$\varepsilon^* = \varepsilon' - i\varepsilon'' = \frac{1}{i\omega C_0 Z^*} \qquad (2)$$

where ω is the angular frequency, and C_0 is the empty cell capacitance.

Figure 6 shows behavior of complex dielectric permittivity at 1 kHz in temperature range from room temperature to 400 ^{o}C. For CCTO_mc ceramics, we found high dielectric permittivity, above 10000, at 1 kHz that is nearly constant from room temperature to 225 ^{o}C. It can be emphasized that CCTO_mc ceramics, especially TSS sample, could be very promising for capacitor applications. CCTO_ss ceramics show smaller dielectric permittivity but also stable in a wide temperature region. As it is previously stressed, a difference in dielectric permittivity between the CCTO ceramics is influenced by different microstructure.

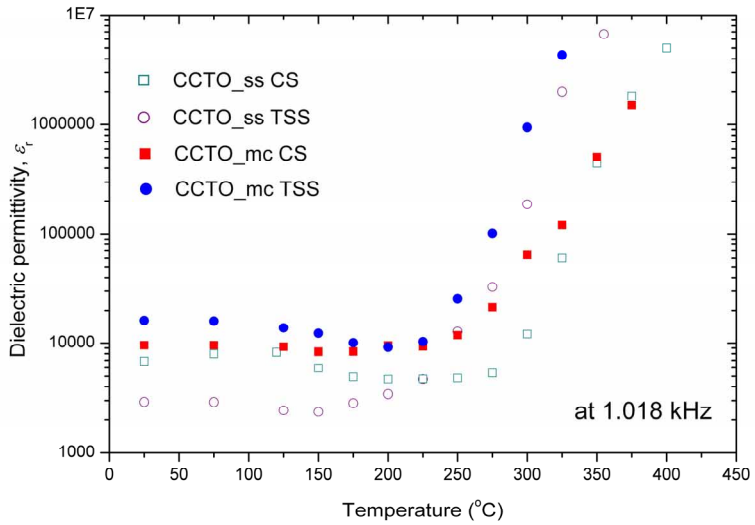

Figure 6. Dependence of dielectric permittivity on temperature, at frequency of 1.018 kHz.

Figure 7 shows the dielectric permittivity of the CCTO samples in the range from 42 Hz to 5 MHz measured at room temperature. It can be observed that dielectric constant decrease with increase of frequency to 1 MHz, while in the range of MHz is quite stable.

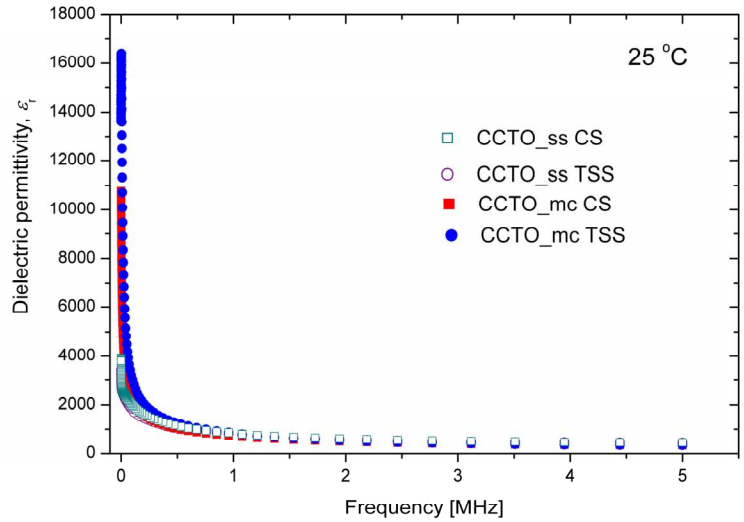

Figure 7. Dependence of dielectric permittivity on frequency measured at room temperature.

The main electrical characteristics of sintered ceramics at room temperature, in MF as well at resonant frequencies are listed in Table II.

Table II. Electrical characteristics of CCTO ceramics.

Sample	Dielectric permittivity at room temperature		Resonant frequency [GHz]	Quality factor [GHz]
	At 1 kHz	At resonant frequency		
CCTO_ss CS	6870	62.2	7.778	4256
CCTO_ss TSS	2917	61.4	6.872	1885
CCTO_mc CS	9566	62.5	7.968	2405
CCTO_mc TSS	16273	64.2	6.773	1310

Thus, according to the IS results, high specific resistivity of the CCTO at room temperature (without leakage currents) in addition to relative permittivity above 16000 at 1 kHz in a wide temperatures interval, make this sintered CCTO ceramics suitable for practical application as capacitors. Besides, the combination of capacitance behavior and high values of dielectric permittivity (above 60) in the MW range confirm the potential use of such materials for preparation of high dielectric planar antennas, with applicability in microelectronics or for microwave devices (for example cell mobile phones), where the miniaturization of the devices is crucial.[14]

In the final stage of this study, we studied the influence of heating regime on microstructure which is correlated with electrical properties. Figure 8 shows microstructure of CCTO ceramics prepared by different heating regimes. It is obvious that heating regimes affected microstructure; it impacts final density as well as average grain size. Estimated values of average grain sizes and final densities are shown in Table I. Here, it can be emphasized that CCTO_mc exhibits bimodal grain size distribution: for CS regime smaller fraction is around 2 μm and larger is around 5 μm; for the TSS regime one fraction is below 1 μm while there are larger grains of several micrometers. In both systems, TSS achieved microstructural refinement, decreasing average grains size for almost 50 %, while density improvement was obtained in the case of CCTO_mc powder. Better response of this powder to TSS method is correlated to powder morphology, much smaller average particle size as well as softer agglomerates, compared to CCTO_ss powder obtained by more severe synthesis conditions. Smaller average grain size of the CCTO_mc compared to CCTO_ss ceramics obtained by both CS and TSS methods influenced the value of dielectric permittivity at 1.018 kHz, which is several times higher. Furthermore, considering CCTO_mc system, average grain size reduction and density improvement obtained in TSS regime yielded to significant increase of dielectric permittivity at 1 kHz value.

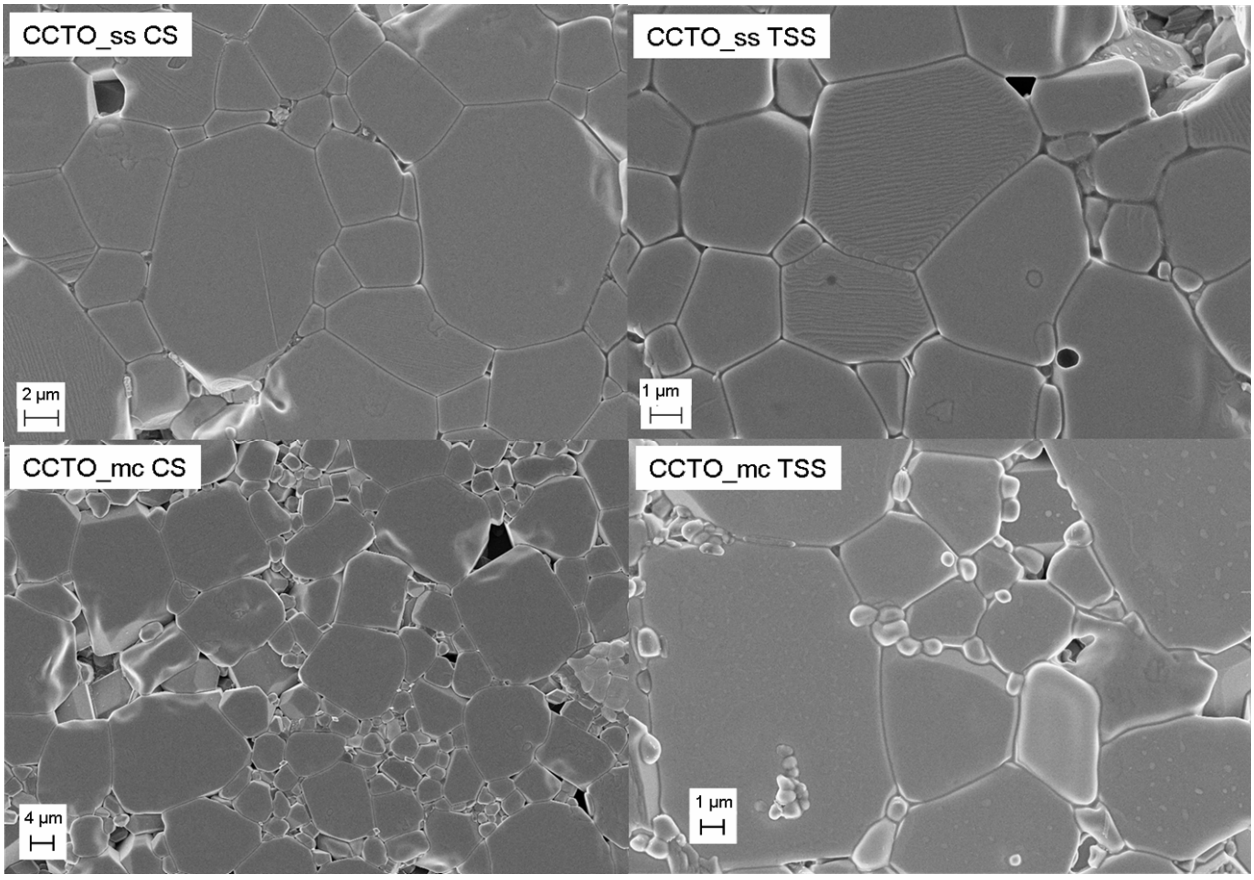

Figure 8. Microstructure of CCTO ceramics prepared from CCTO_ss and CCTO_mc powders by CS and TSS sintering regimes.

In order to confirm that differences in electrical properties of CCTO ceramics are determined by created microstructure rather than by different phase composition, XRD patterns of sintered ceramics are recorded, Figure 9. Obviously, all of the examined electronic ceramics possess the same phase composition corresponding to pure CCTO crystal phase.

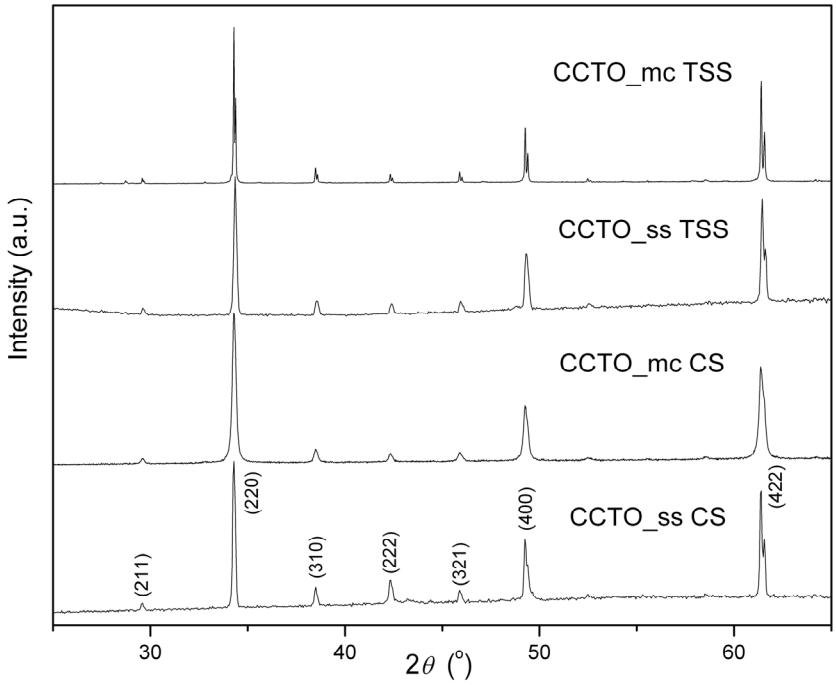

Figure 9. XRD patterns of CCTO ceramics prepared from CCTO_ss and CCTO_mc powders by CS and TSS sintering regimes.

CONCLUSION

CCTO powders with different characteristics were prepared by solid-state (CCTO_ss) and mechanochemical (CCTO_mc) methods. Their sintering behavior was investigated by heating microscopy with different heating rates and it is found that CCTO_mc powder possesses better sinterability which is connected with its more uniform powder morphology and existence of smaller, softly agglomerated particles in spite of CCTO_ss powder, consisting of hard aggregation of a large micrometer sized particles. Based on sintering behavior, experiments of conventional (CS) and two-step sintering (TSS) were carried out. It is shown that in the case of both powders, TSS yielded to microstructural refinement; in addition, for CCTO_mc density increase is found. Furthermore, electrical properties of sintered ceramics were investigated in MF as well in MW region. According to the results of MF measurements, the sintered CCTO ceramics has both, the high specific resistivity at room temperature and high relative permittivity at 1 kHz in a wide temperatures interval, which makes these materials suitable for practical application as capacitors. Besides, high values of dielectric permittivity (above 60) at resonant frequency are measured. The combination of capacitance behavior and high dielectric permittivity in the MW range promote the potential use of such materials for preparation of high dielectric planar antennas, with applicability in microelectronics

XRD measurements of investigated samples confirmed that difference in electrical characteristics is a consequence of microstructural changes rather than that of phase composition

since only present phase in all samples corresponds to pure CCTO crystal phase. This fact emphasized the responsibility of sintering strategy development to prepare appropriate microstructure with desirable electrical properties.

ACKNOWLEDGEMENT

This study was supported by the Ministry of Education and Science of the Republic of Serbia under Grant No. III45004, and the bilateral cooperation program between the Republic of Serbia and the Republic of Slovenia under Grant No. 651-03-1251/2012-09/06.

REFERENCES:

1. M.A. Subramanian, D. Li, N. Duan, B.A. Reisner, A.W. Sleight, High dielectric constant in $ACu_3Ti_4O_{12}$ and $ACu_3Ti_3FeO_{12}$ phases, Journal of Solid State Chemistry 151 (2000) 323–325.
2. J. Liu, R.W. Smith, W.-N. Mei, Synthesis of the giant dielectric constant material $CaCu_3Ti_4O_{12}$ by wet-chemistry methods, Chemistry of Materials 19 (2007) 6020–6024.
3. M.A. De la Rubia, P. Leret, J.bDe Frutos, J.F. Fernández, Effect of the synthesis route on the microstructure and the dielectric behavior of $CaCu_3Ti_4O_{12}$ ceramics, Journal of the American Ceramic Society 95 (2012) 1866–1870
4. D.-L. Sun, A.-Y. Wu, S.-T. Yin, Structure, properties, and impedance spectroscopy of $CaCu_3Ti_4O_{12}$ ceramics prepared by sol–gel process, Journal of the American Ceramic Society 91 (2008) 169–173.
5. S. K. Jo, Y. H. Han, Sintering behavior and dielectric properties of polycrystalline $CaCu_3Ti_4O_{12}$. Journal of Materials Science: Materials in Electronics 20 (2009) 680–684.
6. JCPDS Database on CD-ROM, International Centre for Diffraction Data, Newton Square, PA, 1999.
7. B. Bochu, M.N. Deschizeaux, J.C. Joubert, Synthèse et caractérisation d'une série de titanates pérowskites isotypes de $[CaCu_3](Mn_4)O_{12}$, Journal of Solid State Chemistry 29 (2) (1979) 291–298.
8. S.K. Manik, S.K. Pradhan, Microstructure characterization of ball-mill-prepared nanocrystalline $CaCu_3Ti_4O_{12}$ by Rietveld method, Physica E 33 (2006) 160–168.
9. I.-W. Chen, X.-H. Wang, Sintering dense nanocrystalline ceramics without final-stage grain growth. Nature 404 (2000) 168–171.
10. J.E. Bauerle, Study of solid electrolyte polarization by a complex admittance method, J Phys Chem Solids 30 (1969) 2657–70.
11. N. Hirose, A.R.West, Impedance spectroscopy of undoped BaTiO3 ceramics. J Am Ceram Soc 79 (1996) 1633–41.
12. J.R. Macdonald, editor. Impedance Spectroscopy. New York/Chichester/ Brisbane/Toronto/Singapore: John Wiley & Sons; 1987.
13. S. Marković, Č. Jovalekić, Lj. Veselinović, S. Mentus and D. Uskoković, Electrical properties of barium titanate stannate functionally graded materials, Journal of the European Ceramic Society 30 (2010) 1427–1435.
14. A.F.L. Almeida, P.B.A. Fechine, L.C. Kretly, A.S.B. Sombra, $BaTiO_3$ (BTO)–$CaCu_3Ti_4O_{12}$ (CCTO) substrates for microwave devices and antennas, Journal of Materials Science 41 (2006) 4623–4631.